Free Cooling of a Granular Gas of Rodlike Particles in Microgravity

Kirsten Harth, Torsten Trittel, Sandra Wegner, and Ralf Stannarius
Institute for Experimental Physics, Otto von Guericke University, D-39106 Magdeburg, Germany

(Received 16 November 2017; published 22 May 2018)

Granular gases as dilute ensembles of particles in random motion are at the basis of elementary structure-forming processes in the Universe, involved in many industrial and natural phenomena, and also excellent models to study fundamental statistical dynamics. The essential difference to molecular gases is the energy dissipation in particle collisions. Its most striking manifestation is the so-called granular cooling, the gradual loss of mechanical energy $E(t)$ in the absence of external excitation. We report an experimental study of homogeneous cooling of three-dimensional granular gases in microgravity. The asymptotic scaling $E(t) \propto t^{-2}$ obtained by Haff's minimal model [J. Fluid Mech. **134**, 401 (1983)] proves to be robust, despite the violation of several of its central assumptions. The shape anisotropy of the grains influences the characteristic time of energy loss quantitatively but not qualitatively. We compare kinetic energies in the individual degrees of freedom and find a slight predominance of translational motions. In addition, we observe a preferred rod alignment in the flight direction, as known from active matter or animal flocks.

DOI: 10.1103/PhysRevLett.120.214301

Cars and pedestrians in traffic, migrating groups of animals or bacteria, bubbles in fluid flows, or grains in sand storms are examples of large particle ensembles where occasional interactions of the individual constituents govern the collective dynamics. All these are inherently out of thermal equilibrium. Granular gases, i.e., dilute ensembles of grains interacting by dissipative collisions, represent the simplest of such systems, without long-range interactions. In contrast to molecular gases, the dissipative character of particle interactions determines the ensemble properties: Clustering (e.g., [1–7]), non-Gaussian velocity distributions (e.g., [8–21]), and anomalous pressure scaling [22–24] are but a few documented examples.

But, even today, quantitative experiments are very much needed for a better understanding of the fundamental features of such ensembles. Analytical and numerical studies in the past 20 years produced results strongly depending on the simplifications made and assumptions of specific grain properties (see, e.g., [1,25–32]). Often, spherical grains under ideal initial and boundary conditions were considered. In experiments with quasi-2D layers (e.g., [5–8,10–12,33,34]), energy equipartition [8,33,34] and collisions of particles [35,36] were analyzed in addition to the above-mentioned features.

Most prominent is granular cooling, the permanent loss of kinetic energy in the absence of external forcing. Starting from an initially excited state with spatially homogeneous statistical properties, the ensemble enters an initial period of homogeneous energy loss. At longer time scales, grains can spontaneously cluster. Such clustering is a key ingredient for the formation of planetesimals and larger objects in solar systems [37–40].

For the homogeneous phase, Haff [41] predicted that the mean energy of a freely cooling granular gas of *frictionless spheres* obeys the scaling

$$E(t) = E_0(1 + t/\tau_H)^{-2}, \tag{1}$$

yielding $E(t) \propto t^{-2}$ for $t \gg \tau_H$, with the characteristic Haff time $\tau_H(E_0)$. Haff starts with the dissipation rate $\partial/\partial t(\rho\bar{v}^2/2) = -\xi(1-\varepsilon^2)\rho\bar{v}^3/s$. Here, ρ is the mass density, s is the mean grain separation (in our dilute system to be replaced by the mean free path λ), ε is the normal restitution coefficient, and $\bar{v}$ is the mean absolute velocity. ξ depends upon the dimensionality of the system; it basically accounts for the fact that only the relative velocities (in our system, also rotations) of colliding particles are relevant for the energy loss, which is then redistributed among all degrees of freedom (d.o.f.). Haff assumed that the distance between the grains is small compared to their diameter (a condition relaxed in subsequent work). He set the quantity $\overline{v^2}$ (related to the average kinetic energy) equal to $\bar{v}^2$ (the square of the mean absolute velocity determining the collision rate $\bar{v}/s$).

The Haff time describing cooling after time t_i is

$$\tau_H(t_i) = \lambda[\xi(1-\varepsilon^2)\bar{v}(t_i)]^{-1}. \tag{2}$$

Villemot and Talbot [30] extended this model to gases of frictionless ellipsoids and compared analytical approximations with simulations. Spherocylinders were simulated by Rubio-Largo *et al.* [31]. The aspect ratios in both studies were much smaller than those of our rods. Huthmann, Aspelmeier, and Zippelius [32] explored the limit of

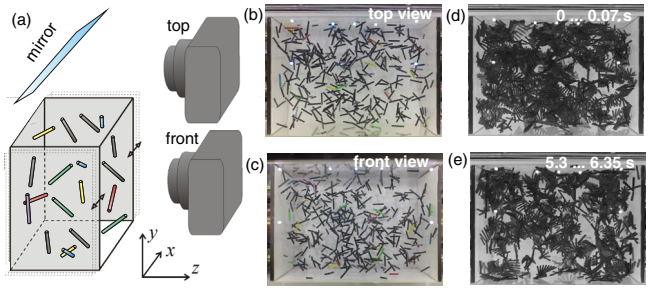

FIG. 1. (a) Sketch of the experimental setup and definition of the coordinates. Two side walls can be vibrated mechanically; the top and front walls are transparent. (b),(c) Typical frames of the top and front videos. Colored particles are tracked, and black rods provide thermal background. (d),(e) Overlay of eight frames of the top view, at the beginning of cooling [(d) homogeneous state] and at the end of the experiment [(e) slight clustering].

infinitely thin needles. All these models confirmed the t^{-2} time dependence of the kinetic energy; corrections concern only the prefactor ξ. Nevertheless, Kanzaki *et al.* [25] found an exponent $-5/3$ for translational d.o.f. from simulations of elongated viscoelastic grains [$\varepsilon(v)$] in 2D. The same exponent was derived rigorously for viscoelastic spheres [42]. In addition, a rather unusual aspect of Kanzaki's simulations is that translational and rotational d.o.f. have *different* scaling exponents.

Preparation of a freely cooling granular gas in 3D is practically impossible under normal gravity. Sounding rockets, satellites, and drop towers offer appropriate conditions [43]: excellent microgravity (μg) quality, down to residual accelerations of 10^{-5} m/s^2. In a pioneering experiment, the dynamical clustering of spheres was reported by Falcon *et al.* [2], but a quantitative analysis at the grain level was not possible for technical limitations. *Rod-shaped* grains offer experimental advantages over spheres: a much shorter mean free path at comparable filling fractions [20], a more random energy injection by vibrating container walls [44], and an efficient energy redistribution among the d.o.f. in collisions [31]. The latter two features can reduce spatial inhomogeneities. Translations and rotations can be followed in 3D [45]. We present results of the first experimental investigation of a homogeneously cooling 3D granular gas.

Ensembles of 374 rods of $\ell = 10$ mm length and $d = 1.35$ mm diameter are studied in a container of 11.2 cm $\times$ 8.0 cm $\times$ 8.0 cm [Figs. 1(a)–1(c)] during $\approx$9 s of microgravity realized in the ZARM Drop Tower, Bremen. The corresponding volume fraction of grains is $\phi = 0.75\%$. The mean free path estimated from the filling fraction and the rod dimensions, assuming random rod orientations, is $\lambda \approx \sqrt{2}d^2/[\phi(\ell + 7.55d + 2.02d^2/\ell)] \approx 1.65$ cm (see [46]), well below the Knudsen regime ($\lambda >$ container size). The rods are custom-made from insulated copper wire, their mass is $m = 37.5$ mg, and moments of inertia for rotations around the rod axis and perpendicular to it are $J_\parallel = 4.6$ pN m s^2 and $J_\perp = 315$ pN m s^2, respectively. The Supplemental video [46] shows one typical experiment. We average 15 independent experiments.

Steady excitation state.—During the initial 2 s of microgravity, the grain ensemble is excited mechanically. In this initial, driven state, one finds an excess of translational energy in the direction of excitation x (normal to the vibrating walls), $\langle E_x(0)\rangle \approx 135$ nJ per grain. Translations in the directions y and z and rotations are only weakly excited by the vibrating walls [44]; they are driven by rod-rod collisions. The indirectly excited y and z translations are equivalent. Initially, $\langle E_y + E_z\rangle/2 \approx$ 90 nJ, and $\langle E_{\rm rot}/2\rangle \approx 64$ nJ for rotations about the short rod axes (these two rotations cannot be distinguished in our experiment; we can only determine their sum $E_{\rm rot}$). Such differences in translation energies in the excitation direction and perpendicular to it are well known (e.g., [17,18,34,47]). As in our previous studies [20,45], we observe a violation of energy equipartition between rotations and translations in the driven state.

Spatial homogeneity during cooling.—After the excitation is stopped ($t = 0$), videos (100 fps) are recorded and a particle-based statistical analysis (see [46]) is performed to evaluate the ensemble dynamics. Throughout the cooling process, we found only a marginal tendency of clustering. This is visualized best by overlaying image sequences from a single experiment. Figures 1(d) and 1(e) show two such overlays. Immediately after t_0, eight subsequent frames of the top video were superimposed [Fig. 1(d)], and the field of view is rather uniformly covered by rods; Fig. 1(e) is a superposition of eight frames from the final phase of the experiment, where every 15th frame was chosen, because the mean velocity is slower by a factor of $\approx$15. One can identify only small inhomogeneities in the particle distribution, which may be neglected here.

Partition of the kinetic energy.—Of primary interest are the energy partition and the energy loss during cooling. Both aspects cannot be discussed separately. After the excitation stopped, the kinetic energy is redistributed by collisions. Thereby, the partition among the d.o.f. changes drastically (Fig. 2). Within statistical fluctuations, a steady distribution of the kinetic energy is reached after $\approx$2…2.5 s [48]. The initial excess of E_x has vanished. The kinetic energies of rotations around the short rod axes remain slightly smaller than those of the translational d.o.f. This is in qualitative agreement with simulations of frictionless ellipsoids [30], rods [31], and needles [32] that predicted an excess of translational over rotational energies per d.o.f. by a few percent.

Rotations around the rod symmetry axis are excited only by frictional contacts of particles in collisions (similar to the rotational d.o.f. of spherical grains [26–28,49]). The ratio of the moments of inertia is $J_\perp/J_\parallel \approx 70$; therefore, such rotations would need to be almost one order of

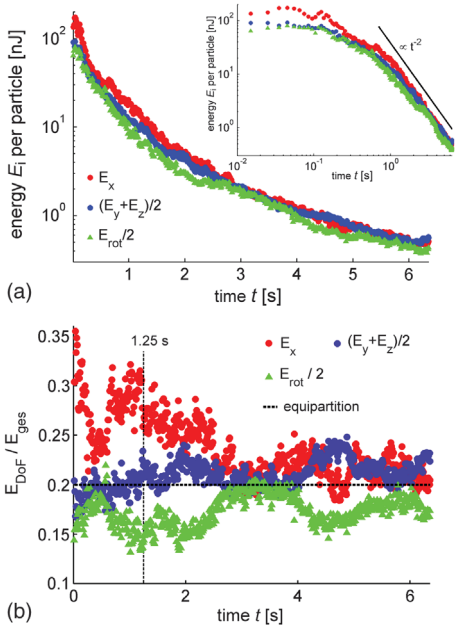

FIG. 2. (a) Decay of the kinetic energy per particle in the individual degrees of freedom: After ≈2.5 s, the energy partition is steady within statistical fluctuations (see Supplemental Material [46]), and the decay proceeds as t^{-2} as predicted by Eq. (1) (see logarithmic plot in the inset). (b) Energies in the different types of d.o.f., all translational d.o.f. equilibrate within statistical fluctuations, rotations about the short rod axes are systematically less excited by about 10%–20%, and the rotations about the long axis were not considered here.

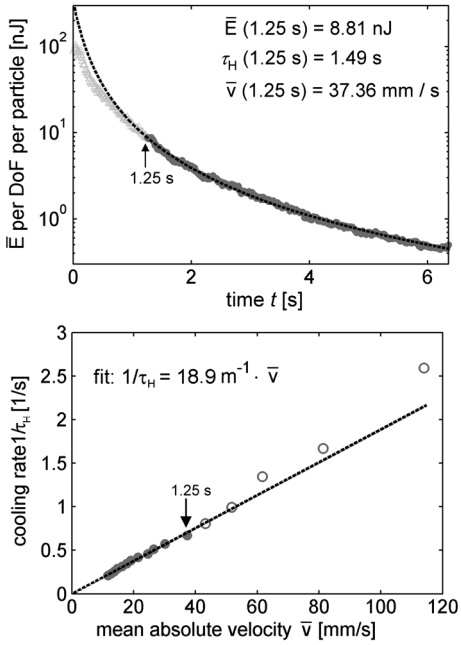

FIG. 3. The cooling characteristics matches Haff's model. (a) Decay of the average kinetic energy per d.o.f. and particle: After ≈1.25 s, the curve is in good agreement with Haff's model [41], Eq. (1) (logarithmic fit). (b) Comparison of the cooling rate and the measured mean velocities. The slope is $\xi(1-\varepsilon^2)/\lambda$. Solid symbols represent the data included in the fits; open symbols correspond to the initial 1.25 s when Haff's equation is not yet applicable.

magnitude faster than the other rotations in equipartition. For an estimate, we marked some rods with dots to track axial rotations to evaluate them quantitatively, albeit with poorer statistics than the other d.o.f. Indeed, the related mean kinetic energy is about one order of magnitude lower than those of the other d.o.f. [50]. The few theoretical studies of elongated grains disregard friction; thus, the third rotation is not included. The other two rotational d.o.f. are directly excited by rod-rod collisions and do not require friction. For rough spheres, models predict a much stronger excitation of rotational d.o.f. compared to translations (e.g., [26,49]). Energy transfer through collisions of rods is much more complex and thus not directly comparable with these models.

The distributions of the velocity components v_x, v_y, and v_z are non-Gaussian. Within statistical accuracy, their shape remains nearly unchanged during the homogeneous cooling. The kurtosis shows no obvious trend, fluctuating between 3 and 4, with an average of 3.5. In contrast, in simulations of both ellipsoids [30] and spherocylinders [31], perfect Gaussian distributions were reported.

Cooling.—During the observation window of about 7 s, the total kinetic energy decays by more than 2 orders of magnitude to ≈0.45 nJ per d.o.f. Checking Haff's precondition, we find experimentally a ratio of $\overline{v^2}$ and $\bar{v}^2$ between 1.2 and 1.32. Data in Fig. 2(a) are in excellent agreement with an exponent −2 for the energy decay. Figure 3(a) shows that Eq. (1) fits the mean total energy after some initial period of ≈1.25 s.

The initial discrepancy is easily understood: Immediately after excitation, the system is spatially inhomogeneous. For example, particles are "hotter" near the vibrating plates. The individual d.o.f. are at very different granular temperatures. Therefore, the Haff fit after 1.25 s [dashed line in Fig. 3(a)] overestimates the initial $E(t)$. After about 1.25 s, the system is in the homogeneous cooling regime. This is confirmed by the mutual dependence of τ_H and $\bar{v}$ [Fig. 3(b)]: Experimental data were fitted with Eq. (1) starting at different $t_i > 0$ during cooling, and the inverse of the fit parameter $\tau_H(t_i)$ was related to the momentary mean absolute velocities $\bar{v}(t_i)$. The linear fit confirms Eq. (2) and yields $\xi = 18.9\ \mathrm{m}^{-1}\lambda/(1-\varepsilon^2)$.

A further test of the model is the measured cumulative collision number per particle

$$N_c = \frac{1}{\xi(1-\varepsilon^2)} \ln\left(1+\frac{t}{\tau_H}\right) + \text{const} \qquad (3)$$

(Fig. 4). The dashed line is a fit for $t > 1.25$ s, yielding $\xi = 0.31/(1-\varepsilon^2)$. Again, the initial values deviate,

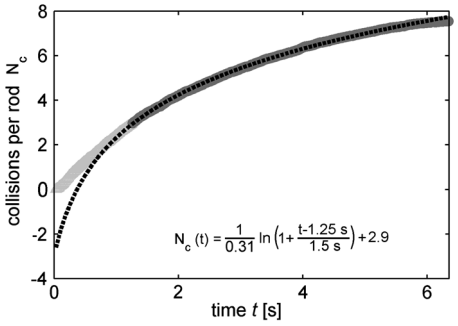

FIG. 4. Cumulated number of collisions per particle determined from the rate of collision of traced (colored) particles in the videos. Only the dark data points were fitted.

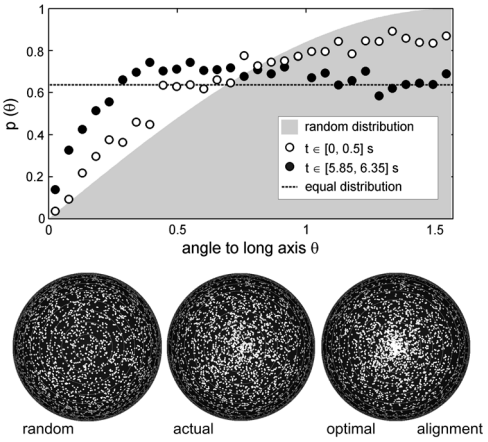

FIG. 5. Angle between the rod symmetry axis and $\vec{v}$ during the initial 0.5 s of cooling and during the last 0.5 s of the experiment. The pictures below illustrate the distribution $p(\theta)$ by bright dots projected on a unit sphere, looking in the flight direction, left: isotropically distributed rod axes, middle: experiment at $t \approx 6$ s, and right: best possible alignment.

partially because the homogeneous cooling is not yet reached and partially because the particles are very fast, so that not all collisions may have been detected (both reflected in the offset). Together with the fit in Fig. 3, we obtain $\lambda = (0.31/18.9)\ \mathrm{m} \approx 1.64$ cm, in excellent agreement with our geometrical estimate of 1.65 cm.

The following complications affect the interpretation of the factor ξ: In Haff's model, the energy loss per collision is distributed among three translational d.o.f., whereas in our system, translational energy is partially converted into rotational energy and vice versa. The loss of rotation energy per collision is much more difficult to estimate than for frictionless spheres. In addition, the mean kinetic energy of rotations about the long rod axis is known only to the order of magnitude. An analytical model [30] and numerical simulations [30,31] provide estimates of ξ. We calculate the collision rate per particle [Eq. (13) in Ref. [30]], approximating our rods by ellipsoids and using the corresponding geometrical parameters: the isotropically averaged contact value of the pair distribution function, $g_c \approx 1.035$, the average exclusion surface $S_c = 25 \times 10^{-6}\ \mathrm{m}^2$, and the effective number of excited d.o.f. of about 5. Shape effects are reflected in a correction factor $\langle D \rangle_c$ describing the average efficiency of energy transfer during a collision, compared to spheres. This value increases from 1 for an aspect ratio of 1 to about 1.4 for ellipsoids with aspect ratio 3 [30]. With our τ_H, we obtain $\langle D \rangle_c = 5.0$, a value much larger than the extrapolation of Villemot's graph, $\langle D \rangle_c \approx 1.75$. Thus, the cooling of rods in our experiment is more efficient by a factor of almost 3. There are several potential explanations for this discrepancy. First, it is not clear whether the predictions for short ellipsoids or spherocylinders can be extrapolated to rods with aspect ratios above 7. Second, the mass distribution along the grain axis substantially affects the energy distribution between translations and rotations [30,32]. Third, the models disregard friction. An additional problem is the preferential alignment of the rods in the flight direction (see below). The scattering cross section of a rod momentarily flying in the long axis direction is much smaller than in the perpendicular orientation. Consequently, the collision characteristics differ, and the transfer of angular momentum will be much smaller on average in the first case.

Alignment.—One particular feature of anisotropic grains is their tendency to align in a shear flow [51]. Correlations between the velocity and orientation were reported in simulations of hard needles [32]. We find similar correlations in the distribution of relative rod orientations $p(\theta)$, where $\theta = 0°$ resembles a spearlike orientation. During excitation, the alignment angles are distributed almost isotropically [$p(\theta) \propto \sin\theta$]. During cooling, rods are more often in a spearlike orientation, and the probability of small θ increases, while it decreases for large θ (Fig. 5). This can be understood intuitively: Rod-rod collisions are more probable when the rod axis is perpendicular to the flight path than in the flight direction. The consequence is a slightly larger λ than estimated for random rod orientations. The effect is small, though, as illustrated in the bottom images in Fig. 5. Note that the highest possible alignment of rotating rods would be an equal distribution $p(\theta) = 2/\pi$ (black line in the image), when all rotations occur about short axes perpendicular to the flight path (like spokes of a wheel).

Correlations between translational and rotational motions were even found in simulations of ensembles of spheres [27,29]. These findings are only loosely related to the described alignment of rods, but both effects influence the collision statistics and are therefore important for realistic models of granular cooling, even in dilute ensembles.

The experimental study of homogeneous free cooling of a 3D granular gas in microgravity demonstrates that Haff's scaling law of the energy loss with time is surprisingly robust, even though several central assumptions are not

fulfilled; e.g., one has friction and shape anisotropy of the grains and non-Gaussian velocity distributions even in the homogeneous cooling state. Quantitatively, the efficiency of cooling is much higher in our experiment than expected from an extrapolation of an analytical model for ellipsoids [30]. Energies become nearly equally distributed among the d.o.f. in the homogeneously cooling state, with a slight excess ($\approx 10\%$–20%) in the translational d.o.f. Even the purely friction-coupled rotations around the long axis are excited, albeit with one order of magnitude lower mean energy. A gradual alignment of rods in the flight direction is also documented, explainable by the lower collision probability in this flight orientation.

The detailed mechanisms underlying the collective dynamics of realistic granular gases, e.g., the exact role of particle shape, contact parameters, confinement, and spatial inhomogeneities, are still to be explored. Beyond fundamental physics, our results provide a robust benchmark for the realistic modeling of dilute granular ensembles, which in turn forms the basis for the description of more complex, dense ensembles. Further quantitative experiments may allow tests of extended models [26,31] which consider the exchange between rotational and translational d.o.f. in detail. In perspective, only the combined efforts of theoretical studies allowing for experimental verification and quantitative experiments may lead to the comprehensive understanding of granular fluids and clarify the links between individual grain collision and ensemble dynamics of granular gases in an extendable and realistic manner.

The authors acknowledge funding by the German Aerospace Center DLR, Projects No. 50WM1241 and No. 50WM1344, and by the German Science Foundation (DFG) Grant No. STA 425/34-1. We cordially thank the ZARM staff in Bremen for their excellent support in the drop tower experiments.

[1] I. Goldhirsch and G. Zanetti, Clustering Instability in Dissipative Gases, Phys. Rev. Lett. **70**, 1619 (1993).
[2] E. Falcon, R. Wunenburger, P. Évesque, S. Fauve, C. Chabot, Y. Garrabos, and D. Beysens, Cluster Formation in a Granular Medium Fluidized by Vibrations in Low Gravity, Phys. Rev. Lett. **83**, 440 (1999).
[3] E. Opsomer, F. Ludewig, and N. Vandewalle, Phase transitions in vibrated granular systems in microgravity, Phys. Rev. E **84**, 051306 (2011).
[4] M. Hummel, J. P. D. Clewett, and M. G. Mazza, A universal scaling law for the evolution of granular gases, Europhys. Lett. **114**, 10002 (2016).
[5] A. Kudrolli, M. Wolpert, and J. P. Gollub, Cluster Formation due to Collisions in Granular Material, Phys. Rev. Lett. **78**, 1383 (1997).
[6] C. C. Maaß, N. Isert, G. Maret, and C. M. Aegerter, Experimental Investigation of the Freely Cooling Granular Gas, Phys. Rev. Lett. **100**, 248001 (2008).
[7] J. C. Burton, P. Y. Lu, and S. R. Nagel, Energy Loss at Propagating Jamming Fronts in Granular Gas Clusters, Phys. Rev. Lett. **111**, 188001 (2013).
[8] K. Nichol and K. E. Daniels, Equipartition of Rotational and Translational Energy in a Dense Granular Gas, Phys. Rev. Lett. **108**, 018001 (2012).
[9] M. Hou, R. Liu, G. Zhai, Z. Sun, K. Lu, Y. Garrabos, and P. Evesque, Velocity distribution of vibration-driven granular gas in Knudsen regime in microgravity, Microgravity Sci. Technol. **20**, 73 (2008).
[10] J. S. Olafsen and J. S. Urbach, Clustering, Order, and Collapse in a Driven Granular Monolayer, Phys. Rev. Lett. **81**, 4369 (1998).
[11] J. S. Olafsen and J. S. Urbach, Velocity distributions and density fluctuations in a granular gas, Phys. Rev. E **60**, R2468 (1999).
[12] S. Tatsumi, Y. Murayama, H. Hayakawa, and M. Sano, Experimental study on the kinetics of granular gases under microgravity, J. Fluid Mech. **641**, 521 (2009).
[13] A. Kudrolli and J. Henry, Non-Gaussian velocity distributions in excited granular matter in the absence of clustering, Phys. Rev. E **62**, R1489 (2000).
[14] M. Schmick and M. Markus, Gaussian distributions of rotational velocities in a granular medium, Phys. Rev. E **78**, 010302 (2008).
[15] I. S. Aranson and J. S. Olafsen, Velocity fluctuations in electrostatically driven granular media, Phys. Rev. E **66**, 061302 (2002).
[16] F. Rouyer and N. Menon, Velocity Fluctuations in a Homogeneous 2D Granular Gas in Steady State, Phys. Rev. Lett. **85**, 3676 (2000).
[17] C. Huan, X. Yang, D. Candela, R. W. Mair, and R. L. Walsworth, NMR experiments on a three-dimensional vibrofluidized granular medium, Phys. Rev. E **69**, 041302 (2004).
[18] G. Costantini, U. M. B. Marconi, G. Kalibaeva, and G. Cicotti, The inelastic hard dimer gas: A nonspherical model for granular matter, J. Chem. Phys. **122**, 164505 (2005).
[19] R. D. Wildman, J. Beecham, and T. L. Freeman, Granular dynamics of a vibrated bed of dumbbells, Eur. Phys. J. Spec. Top. **179**, 5 (2009).
[20] K. Harth, U. Kornek, T. Trittel, U. Strachauer, S. Höme, K. Will, and R. Stannarius, Granular Gases of Rod-Shaped Grains in Microgravity, Phys. Rev. Lett. **110**, 144102 (2013).
[21] C. Scholz and T. Pöschel, Velocity Distribution of a Homogeneously Driven Two-Dimensional Granular Gas, Phys. Rev. Lett. **118**, 198003 (2017).
[22] P. Evesque, D. Beysens, and Y. Garrabos, Mechanical behaviour of granular-gas and heterogeneous-fluid systems submitted to vibrations in microgravity, J. Phys. IV (France) **11**, Pr6-49 (2001).
[23] J. C. Geminard and C. Laroche, Pressure measurement in two-dimensional horizontal granular gases, Phys. Rev. E **70**, 021301 (2004).
[24] E. Falcon, S. Aumaître, P. Évesque, F. Palencia, C. Lecoutre-Chabot, S. Fauve, D. Beysens, and Y. Garrabos, Collision statistics in a dilute granular gas fluidized by vibrations in low gravity, Europhys. Lett. **74**, 830 (2006).

[25] T. Kanzaki, R. C. Hidalgo, D. Maza, and I. Pagonabarraga, Cooling dynamics of a granular gas of elongated particles, J. Stat. Mech. (2010) P06020.
[26] S. Luding, M. Huthmann, S. McNamara, and A. Zippelius, Homogeneous cooling of rough, dissipative particles: Theory and simulations, Phys. Rev. E **58**, 3416 (1998).
[27] M. Huthmann and A. Zippelius, Dynamics of inelastically colliding rough spheres: Relaxation of translational and rotational energy, Phys. Rev. E **56**, R6275 (1997).
[28] O. Herbst, R. Cafiero, A. Zippelius, H. J. Herrmann, and S. Luding, A driven two-dimensional granular gas with Coulomb friction, Phys. Fluids **17**, 107102 (2005).
[29] N. V. Brilliantov, T. Pöschel, W. T. Kranz, and A. Zippelius, Translations and Rotations Are Correlated in Granular Gases, Phys. Rev. Lett. **98**, 128001 (2007).
[30] F. Villemot and J. Talbot, Homogeneous cooling of hard ellipsoids, Granular Matter **14**, 91 (2012).
[31] S. M. Rubio-Largo, F. Alonso-Marroquin, T. Weinhart, S. Luding, and R. C. Hidalgo, Homogeneous cooling state of frictionless rod particles, Physica (Amsterdam) **443A**, 477 (2016).
[32] M. Huthmann, T. Aspelmeier, and A. Zippelius, Granular cooling of hard needles, Phys. Rev. E **60**, 654 (1999).
[33] L. J. Daniels, Y. Park, T. C. Lubensky, and D. J. Durian, Dynamics of gas-fluidized rods, Phys. Rev. E **79**, 041301 (2009).
[34] K. Feitosa and N. Menon, Breakdown of Energy Equipartition in a 2D Binary Vibrated Granular Gas, Phys. Rev. Lett. **88**, 198301 (2002).
[35] M. Leconte *et al.*, Microgravity experiments on vibrated granular gases in a dilute regime: Non-classical statistics, J. Stat. Mech. (2006) P07012.
[36] M. Montaine, M. Heckel, C. Krülle, T. Schwager, and T. Pöschel, Coefficient of restitution as a fluctuating quantity, Phys. Rev. E **84**, 041306 (2011).
[37] G. Wurm and J. Blum, Experiments on preplanetary dust aggregation, Icarus **132**, 125 (1998).
[38] A. Johansen, J. S. Oishi, M. M. Mac Low, H. Klahr, and T. Henning, Rapid planetesimal formation in turbulent circumstellar disks, Nature (London) **448**, 1022 (2007).
[39] J. P. Williams and L. A. Cieza, in Protoplanetary Disks and Their Evolution, *Annu. Rev. Astron. Astrophys.* Vol. 49, edited by S. M. Faber and E. VanDishoeck (Annual Reviews, Palo Alto, 2011), pp. 67–117.
[40] R. Weidling, C. Güttler, and J. Blum, Free collisions in a microgravity many-particle experiment. I. Dust aggregate sticking at low velocities, Icarus **218**, 688 (2012).
[41] P. K. Haff, Grain flow as a fluid-mechanical phenomenon, J. Fluid Mech. **134**, 401 (1983).
[42] T. Schwager and T. Pöschel, Coefficient of normal restitution of viscous particles and cooling rate of granular gases, Phys. Rev. E **57**, 650 (1998).
[43] K. Harth, T. Trittel, K. May, S. Wegner, and R. Stannarius, Three-dimensional (3D) experimental realization and observation of a granular gas in microgravity, Adv. Space Res. **55**, 1901 (2015).
[44] T. Trittel, K. Harth, and R. Stannarius, Mechanical excitation of rodlike particles by a vibrating plate, Phys. Rev. E **95**, 062904 (2017).
[45] K. Harth, T. Trittel, U. Kornek, S. Höme, K. Will, U. Strachauer, and R. Stannarius, Microgravity experiments on a granular gas of elongated grains, AIP Conf. Proc. **1542**, 807 (2013).
[46] See Supplemental Material at http://link.aps.org/supplemental/10.1103/PhysRevLett.120.214301 for a video of one experimental run, details of data evaluation, estimate of the mean free path and an analysis of statistical uncertainties.
[47] C. Yanpei, P. Evesque, M. Hou, C. Lecoutre, F. Palencia, and Y. Garrabos, Long range boundary effect of 2D intermediate number density vibro-fluidzed granular media in micro-gravity, J. Phys. Conf. Ser. **327**, 012033 (2011).
[48] The role of the uncertainty of our evaluation method and of intrinsic fluctuations of the mean energy is discussed in Supplemental Material [46].
[49] S. McNamara and J. L. Barrat, Energy nonequipartition in systems of inelastic, rough spheres, Phys. Rev. E **58**, 2247 (1998).
[50] In molecular two-atomic gases at room temperature, such rotations about the axis with the smallest moment of inertia are not excited for quantum mechanical reasons.
[51] T. Börzsönyi and R. Stannarius, Granular materials composed of shape-anisotropic grains, Soft Matter **9**, 7401 (2013).